

Capacity limits of systems employing multiple optical phase conjugators

A. D. Ellis,* M. E. McCarthy, M. A. Z. Al-Khateeb, and S. Sygletos

Aston Institute of Photonic Technology, Aston University, Birmingham B4 7ET, UK

*andrew.ellis@aston.ac.uk

Abstract: We extend the theory of parametric noise amplification to the case of transmission systems employing multiple optical phase conjugators, demonstrating that the excess noise due to this process may be reduced in direct proportion to the number of phase conjugation devices employed. We further identify that the optimum noise suppression is achieved for an odd number of phase conjugators, and that the noise may be further suppressed by up to 3dB by partial digital back propagation (or fractional spans at the ends of the links).

©2015 Optical Society of America

OCIS codes: (060.0060) Fiber optics and optical communications; (190.4370) Nonlinear optics, fibers.

References and links

1. D. Qian, M.-F. Huang, E. Ip, Y.-K. Huang, Y. Shao, J. Hu, and T. Wan, "101.7-Tb/s (370×294-Gb/s) PDM-128QAM-OFDM transmission over 3×55-km SSMF using pilot-based phase noise mitigation," in *Optical Fiber Communications Conference*, (OSA, 2011), paper PDPB5.
2. X. Zhou, L. E. Nelson, P. Magill, R. Isaac, B. Zhu, D. W. Peckham, P. I. Borel, and K. Carlson, "PDM-nyquist-32QAM for 450-Gb/s per-channel WDM transmission on the 50 GHz ITU-T Grid," *J. Lightwave Technol.* **30**(4), 553–559 (2012).
3. J.-X. Cai, Y. Cai, C. R. Davidson, A. Lucero, H. Zhang, D. G. Foursa, O. V. Sinkin, W. W. Patterson, A. Pilipetskii, G. Mohs, and N. S. Bergano, "20 Tbit/s capacity transmission over 6,860km," in *Optical Fiber Communications Conference* (OSA, 2011), paper PDPB4.
4. P. P. Mitra and J. B. Stark, "Nonlinear limits to the information capacity of optical fibre communications," *Nature* **411**(6841), 1027–1030 (2001).
5. X. Chen and W. Shieh, "Closed-form expressions for nonlinear transmission performance of densely spaced coherent optical OFDM systems," *Opt. Express* **18**(18), 19039–19054 (2010).
6. P. Poggiolini, "Modeling of non-linear propagation in uncompensated coherent systems," in *Optical Fiber Communications Conference* (OSA, 2013), paper OT3G1.
7. D. Rafique, J. Zhao, and A. D. Ellis, "Digital back-propagation for spectrally efficient WDM 112 Gbit/s PM-ary QAM transmission," *Opt. Express* **19**(6), 5219–5224 (2011).
8. M. D. Pelusi, "Fiber looped phase conjugation of polarization multiplexed signals for pre-compensation of fiber nonlinearity effect," *Opt. Express* **21**(18), 21423–21432 (2013).
9. G. Liga, T. Xu, A. Alvarado, R. I. Killely, and P. Bayvel, "On the performance of multichannel digital backpropagation in high-capacity long-haul optical transmission," *Opt. Express* **22**(24), 30053–30062 (2014).
10. X. Liu, A. R. Chraplyvy, P. J. Winzer, R. W. Tkach, and S. Chandrasekhar, "Phase-conjugated twin waves for communication beyond the Kerr nonlinearity limit," *Nat. Photonics* **7**(7), 560–568 (2013).
11. I. D. Phillips, M. Tan, M. F. C. Stephens, M. E. McCarthy, E. Giacomidis, S. Sygletos, P. Rosa, S. Fabbri, S. T. Le, T. Kanesan, S. K. Turitsyn, N. J. Doran, P. Harper, and A. D. Ellis, "Exceeding the nonlinear-Shannon limit using Raman laser based amplification and optical phase conjugation," in *Optical Fiber Communications Conference* (OSA, 2014), paper M3C1.
12. S. Kilmurray, T. Fehenberger, P. Bayvel, and R. I. Killely, "Comparison of the nonlinear transmission performance of quasi-Nyquist WDM and reduced guard interval OFDM," *Opt. Express* **20**(4), 4198–4205 (2012).
13. A. D. Ellis, J. Zhao, and D. Cotter, "Approaching the non-linear Shannon limit," *J. Lightwave Technol.* **28**(4), 423–433 (2010).
14. D. Rafique and A. D. Ellis, "Impact of signal-ASE four-wave mixing on the effectiveness of digital back-propagation in 112 Gb/s PM-QPSK systems," *Opt. Express* **19**(4), 3449–3454 (2011).
15. T. Tanimura, M. Nölle, J. K. Fischer, and C. Schubert, "Analytical results on back propagation nonlinear compensator with coherent detection," *Opt. Express* **20**(27), 28779–28785 (2012).
16. G. Gao, X. Chen, and W. Shieh, "Influence of PMD on fiber nonlinearity compensation using digital back propagation," *Opt. Express* **20**(13), 14406–14418 (2012).

17. A. D. Ellis, M. A. Sorokina, S. Sygletos, and S. K. Turitsyn, "Capacity limits in nonlinear fiber transmission," in *Asia Communications and Photonics Conference* (OSA, 2013), paper AW4F.1.
18. L. B. Du, M. M. Morshed, and A. J. Lowery, "Fiber nonlinearity compensation for OFDM super-channels using optical phase conjugation," *Opt. Express* **20**(18), 19921–19927 (2012).
19. H. Hu, R. M. Jopson, A. Gnauck, M. Dinu, S. Chandrasekhar, X. Liu, C. Xie, M. Montoliu, S. Randel, and C. McKinstrie, "Fiber nonlinearity compensation of an 8-channel WDM PDM-QPSK signal using multiple phase conjugations," in *Optical Fiber Communications Conference* (OSA, 2014), paper M3C.2.
20. I. Sackey, F. Da Ros, M. Jazayerifar, T. Richter, C. Meuer, M. Nölle, L. Molle, C. Peucheret, K. Petermann, and C. Schubert, "Kerr nonlinearity mitigation in 5×28 -GBd PDM 16-QAM signal transmission over a dispersion-uncompensated link with backward-pumped distributed Raman amplification," *Opt. Express* **22**(22), 27381–27391 (2014).
21. K. Solis-Trapala, M. D. Pelusi, H. N. Tan, T. Inoue, and S. Namiki, "Transmission optimized impairment mitigation by 12 Stage phase conjugation of WDM 24x48 Gb/s DP-QPSK signals," in *Optical Fiber Communications Conference*, (OSA, 2015), paper Th3C.2.
22. K. Solis-Trapala, T. Inoue, and S. Namiki, "Nearly-ideal optical phase conjugation based nonlinear compensation system," in *Optical Fiber Communications Conference*, (OSA, 2014), paper W3F.8.
23. M. H. Shoreh, "Compensation of nonlinearity impairments in coherent optical OFDM systems using multiple optical phase conjugate modules," *J. Opt. Commun. Netw.* **6**(6), 549–558 (2014).
24. M. Morshed, L. B. Du, B. Foo, M. D. Pelusi, B. Corcoran, and A. J. Lowery, "Experimental demonstrations of dual polarization CO-OFDM using mid-span spectral inversion for nonlinearity compensation," *Opt. Express* **22**(9), 10455–10466 (2014).
25. I. Sackey, F. Da Ros, J. K. Fischer, T. Richter, M. Jazayerifar, C. Peucheret, K. Petermann, and C. Schubert, "Kerr nonlinearity mitigation: mid-link spectral inversion versus digital backpropagation in 5×28 -GBd PDM 16-QAM signal transmission," *J. Lightwave Technol.* **33**(9), 1821–1827 (2015).
26. A. D. Ellis, S. T. Le, M. A. Z. Al-Khateeb, S. K. Turitsyn, G. Liga, D. Lavery, T. Xu, and P. Bayvel, "The impact of phase conjugation on the nonlinear-Shannon limit," presented at IEEE Summer Topical Meeting on Nonlinear Optical Signal Processing, Nassau, Bahamas, 13–15th July 2015.
27. D. A. Cleland, C. H. F. Sturrock, and A. D. Ellis, "Precise modelling of four wave mixing products over 400km of step index fibre," *Electron. Lett.* **28**(12), 1171–1172 (1992).
28. S. T. Le, M. E. McCarthy, N. Mac Suibhne, M. A. Z. Al-Khateeb, E. Giacomidis, N. J. Doran, A. D. Ellis, and S. K. Turitsyn, "Demonstration of phase-conjugated subcarrier coding for fiber nonlinearity compensation in CO-OFDM transmission," *J. Lightwave Technol.* **33**(11), 2206–2212 (2015).
29. M. E. Marhic, *Fiber Optical Parametric Amplifiers, Oscillators and Related Devices*, (Cambridge University, 2008).
30. D. Rafique and A. D. Ellis, "Nonlinearity compensation in multi-rate 28 Gbaud WDM systems employing optical and digital techniques under diverse link configurations," *Opt. Express* **19**(18), 16919–16926 (2011).
31. R. Maher, T. Xu, L. Galdino, M. Sato, A. Alvarado, K. Shi, S. J. Savory, B. C. Thomsen, R. I. Killey, and P. Bayvel, "Spectrally shaped DP-16QAM super-channel transmission with multi-channel digital back-propagation," *Sci. Rep.* **5**, 8214 (2015).
32. P. Poggiolini, A. Carena, Y. Jiang, G. Bosco, V. Curri, and F. Forghieri, "Impact of low-OSNR operation on the performance of advanced coherent optical transmission systems," in *European Conference on Optical Communications* (Systematic, 2014), paper Mo.4.3.2.
33. E. Agrell, A. Alvarado, G. Durisi, and M. Karlsson, "Capacity of a nonlinear optical channel with finite memory," *J. Lightwave Technol.* **32**(16), 2862–2876 (2014).

1. Introduction

Recently reported optical communication experiments have been operating close to the proposed nonlinear Shannon limit for a number of years [1–3]. The nonlinear limit assumes that the intensity dependent refractive index causes co-propagating wavelength division multiplexed (WDM) channels to add multiplicative noise to a channel of interest at a level which scales cubically with the signal power, following the third order nonlinear susceptibility tensor. Various calculation methods have been proposed, including cross phase modulation for widely spaced channels [4], and four-wave mixing for OFDM [5] and single carrier [6] signals. In certain circumstances, numerical simulations have shown that this deterministic nonlinear crosstalk may be compensated at least in principle [7–10], and experimental confirmation of this is beginning to emerge [10–12]. Beyond the nonlinear Shannon limit caused by inter channel nonlinear effects [13], it is believed that parametric noise amplification will limit system performance [14–16]. Note that each amplifier contributes independent amplified spontaneous emission and that it is impossible to separate the amplified spontaneous emission from any given amplifier in an amplifier cascade. Consequently it is particularly difficult to fully compensate for parametric noise

amplification. The apparent inability to compensate for this additional nonlinear noise source by any form of transponder based signal processing has led to a proposed maximum potential benefit for nonlinearity compensation [17] of slightly over 50% improvement in the system capacity (or of the signal-to-noise ratio in dB). Parametric noise amplification is particularly debilitating for long haul networks, where the lower OSNR would prompt interest in nonlinearity compensation, since it scales at least quadratically with the system length. Whilst commercial interest in practically implementable forms of nonlinearity compensation is evident, it is difficult to image that a meagre 50% increase in capacity would significantly postpone the “capacity crunch”.

Recently, there has been a resurgence of interest in an inline form of nonlinearity compensation, optical phase conjugation (OPC) [8,11,18–25]. This all optical technique provides compensation of both intra and inter channel nonlinear effects. Since a single OPC device processes many wavelengths simultaneously, it potentially offers a more energy efficient means of nonlinearity compensation than digital signal processing. Whilst some reports have shown negligible benefits, those which configure the system to maximize the transmission symmetry in power [20,21] and dispersion [22] have shown that significant improvements in performance may be achieved. However, few works have studied the impact of cascades on OPCs on overall system performance [19,21,22]. In these experiments, total data rates of around 1 Tbit/s have been transmitted over substantial differences using Raman amplification to improve power symmetry, and increases in nonlinear threshold of more than 6dB have been observed. However, these increases in nonlinear threshold did not appear to translate into similarly impressive performance gains, either due to excess noise added by the OPC devices, or from other nonlinear effects such as parametric noise amplification.

In this paper we develop a simple, fully closed form expression for the signal to noise ratio of a long haul transmission system employing one or more symmetrically placed OPCs which will allow the maximum potential benefit from multiple OPCs to be determined. Initially, in order to establish this benefit, we assume ideal OPC compensation. That is, we assume that stochastic effects other than amplified spontaneous emission (ASE), such as polarization mode dispersion [26] and polarization dependent loss, are either negligible or automatically compensated at each OPC. Furthermore, we assume that a symmetric power profile is achieved using either a short amplifier spacing or Raman amplification [21] and that third order dispersion is negligible. Our ideal analytical theory is directly verified by numerical simulations, confirming that signal to noise ratio’s may be improved in direct proportion to the number of OPC devices deployed enabling significant increases in signal to noise ratio.

2. Analysis

A closed form expression for the nonlinear noise power spectral density resulting from inter channel nonlinearity and parametric noise amplification [7,16] has been previously calculated based on integration of the quasi phase matched four wave mixing efficiency equations for periodically amplified systems [27] following the method used to derive the system capacity of an OFDM system [5].

$$SNR_0 = \frac{P_s}{NP_N + \eta \log\left(\frac{B^2}{2f_w^2}\right)\left(NP_s^3 + \sum_{n=1}^N nP_s^2 P_N\right) + \eta \sum_{n=1}^N \left(\frac{n}{\pi} + \frac{2}{\alpha L}\{n \text{Log}(n) - n + 1\}\right) P_s^2 P_N} \quad (1)$$

where P_s represents the signal power spectral density, N the number of spans, P_N the noise power spectral density added by each span, η a nonlinear scaling coefficient, B the signal bandwidth, f_w the characteristic phase matching frequency of the fiber, α the loss coefficient and L the span length. Terms in the denominator represent amplified spontaneous emission, weakly phase matched nonlinear interactions and strongly phase matched interaction respectively. Note that typically, the logarithm multiplying the second term in the

denominator would be range between 1.5 and 10 for a single channel and fully populated WDM system respectively. Consequently the strongly phase matched terms are usually neglected by dropping the third term in the denominator [14–16].

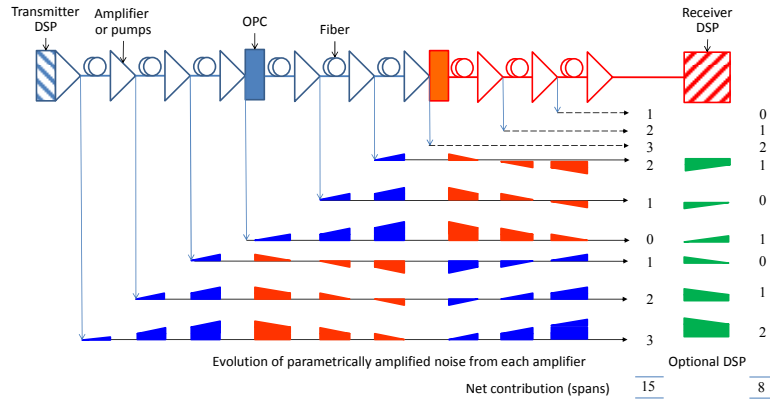


Fig. 1. Principle of the reduction of parametric noise amplification through repeated optical phase conjugation showing; top row, a typical transmission link comprising electronic pre-distortion, amplifiers and fibres, OPC devices and electronic post compensation; lower rows show the evolution of parametrically amplified noise contribution from each amplifier (normalized to the signal power) along the transmission link where blue or red indicates normal or conjugated signal respectively. Each row represents the parametrically amplified noise from a single amplifier. The first column of numbers illustrates the absolute magnitudes of the parametrically amplified noise contribution from each amplifier (normalized to that of a single span) at the output of the link. The green trapezoids indicate the virtual parametric noise amplification added during electronic post compensation of a single span and the second column the (lower) parametrically amplified noise contribution from each amplifier after DSP. Parametrically amplified noise from last three spans not shown.

This model forms the basis for our analysis. Assume that the deterministic nonlinear term proportional to the cube of the signal power may be ideally compensated and consider a long haul transmission system comprising a number of OPC devices separated by amplified segments, as shown in Fig. 1. Without OPC, noise from each amplifier is parametrically amplified by the signals during subsequent transmission along the remainder of the link. The contributions from each amplifier arise from independent ASE sources, and so are summed as independent random variables giving rise to the terms in the denominator of Eq. (1) proportional to $P_S^2 P_N$. Now consider adding OPC at some point along the link (or apply digital back propagation). For the first amplifier in the link, the signal and the ASE are indistinguishable for the rest of the link, so the compensation of nonlinearity after OPC enjoyed by the signal will also be enjoyed by the ASE from the first amplifier. Consequently the parametric noise amplification of the noise arising from the transmitter ASE is fully compensated. For the blue section of the link in Fig. 1 this cancellation is complete as shown in the first row of ASE amplitudes below the system schematic. Unfortunately, for any successive amplifiers in the same segment, this ideal compensation is completed before the end of the link, after this point, further parametric noise amplification begins to degrade the signal to noise ratio. The same argument applies to the response of any pair of identical OPC segments. An arbitrary input to the pair is conjugated and accumulates nonlinear effects in the first segment, re-conjugated whereupon the nonlinearity in the first segment is reversed (assuming ideal OPC). Any field input to the pair of segments is therefore only degraded by the ASE noise added by the two segments. In a practical system, the segments need not be adjacent to each other, but should have the same accumulated dispersion. For uniformly spaced OPCs, this corresponds to a signal launched from the transmitter in Fig. 1, with the

nonlinearity of the two blue segments cancelling exactly. At the receiver the signal is only degraded by nonlinear effects in the final (orange) segment.

In order to calculate the parametric noise amplification for the ASE from each amplifier, we may perform a summation over the number of conjugated on non-conjugated spans, where a conjugated span following a given addition of noise compensates for the parametric noise amplification in a non-compensated span. For simplicity, we consider here the special case of uniformly spaced OPCs. A more direct analytical solution may be obtained however by considering two cases; (1) where the amplifier is followed by an even number of OPC segments, where we need only calculate the parametric noise amplification arising from the segment including the amplifier itself, and (2) where the amplifier is followed by an odd number of OPC segments where we calculate the parametric noise amplification arising from the segment including the amplifier plus the final conjugated segment. The first case is illustrated by the first set of three lines in Fig. 1, where the normalized parametrically amplified noise field first grows, then following OPC is compensated (and, for all but the ASE from the first amplifier, overcompensated) and after the final OPC regrows. The amplitudes are identical to those at the output of the first segment. The second set of three lines represents the second case, where the parametric noise amplification from the first amplifier of the segment in question is ideally compensated, but the remaining amplifiers are overcompensated resulting in a finite parametrically amplified noise field. Of course, for an even number of OPC's, the nonlinear impairment in one segment would be uncompensated and so we assume broadband digital nonlinearity compensation, split between the transmitter (which does not impact the parametric noise amplification) and the receiver (which compensates or over compensates the parametric noise amplification, as shown in Fig. 1). To maintain generality, we assume that DBP may be performed over a fraction of one span. Note however that digital back propagation will initially assist un-conjugated signals (and degraded conjugated signals) and that, as is the case for a transmission segment, may over compensate the contributions from some amplifiers. Following these arguments, it is trivial to show that the parametrically amplified noise field is given by

$$P_{PAN} = \eta P_S^2 P_N \left(N_{Even} \sum_{s=1}^{N_E} f(|s - N_d|) + N_{Odd} \sum_{s=1}^{N_S} f(|s - N_S + N_d|) \right) \quad (2)$$

Where $f(.)$ represents the efficiency of the parametric noise amplification process, N_{Even} and N_{Odd} representing how many even and odd numbered segments are present and N_d the number of spans compensated for digitally in the receiver. Of course, digital back propagation over the full signal bandwidth is largely held to be impractical. We therefore divide the signal spectrum into a narrowband section of width B_{DBP} which may be practically processed digitally and the residual section where the nonlinearity may only be compensated for optically ($N_d = 0$ in Eq. (2)) and sum the resultant contributions. Assuming that the digital back propagation bandwidth is sufficient to capture in full the strongly phase matched contributions, for these two cases, the weighting factors $f(.)$ may be calculated by summing parametric noise amplification contributions, in the case of uniformly spaced OPCs they are given by

$$f_n(s) = \text{Log} \left(\frac{B_{DBP}^2}{2f_w^2} \right) s + \frac{s}{\pi} + \frac{2}{\alpha L} (s \text{Log}(s) - s + 1) \quad (3)$$

and

$$f_b(s) = \text{Log} \left(\frac{B_{WDM}^2}{2f_w^2} \right) s - \text{Log} \left(\frac{B_{DBP}^2}{2f_w^2} \right) s \quad (4)$$

respectively and where the subscripts “n” and “b” refer to the narrow and broadband contributions to $f(s)$ ($f(s) = f_n(s) + f_b(s)$). It is both computationally advantageous and physically insightful to analytically perform the summations in Eq. (2). Following a procedure of further subdividing the summations of Eq. (2) into contributions which are partially, exactly and over compensated and gathering terms in accordance with their length dependence, we find that Eq. (2) may be expressed using the following matrices;

$$\underline{S} = \left(\frac{N_{Even} + N_{Odd}}{2}, N_{Even} - N_{Odd}, N_{Even}, N_{Odd} \right)$$

$$\underline{D} = \begin{pmatrix} N_S^2 & 2(N_D^2 - N_D N_S), & 2N_S \\ \frac{N_S}{2} & -N_D & 0 \\ 0 & 0 & \mathbb{H}(N_d - 1) + \mathbb{H}(N_S - N_d) \\ 0 & 0 & \mathbb{H}(N_d) + \mathbb{H}(N_S - N_d - 1) \end{pmatrix} \quad (5)$$

$$\underline{E} = \left(\log \left(\frac{B_{WDM}^2}{2f_w^2} \right) + \frac{1}{\pi} - \frac{2}{\alpha L}, \log \left(\frac{B_{DBP}^2}{2f_w^2} \right) + \frac{1}{\pi} - \frac{2}{\alpha L}, \frac{2}{\alpha L}, \frac{2}{\alpha L} \right)^T$$

where $\mathbb{H}(\cdot)$ represents the natural logarithm of the Hyper-Factorial function, the vector \underline{S} represents the length scaling rules, the vector \underline{E} the efficiency by which the parametrically amplified noise is generated in the transmission fibre and compensated in DBP, the matrix \underline{D} the system configuration, N_S the number of spans per OPC section, where the total number of spans is given by $N_T = N_S (N_{OPC} + 1)$, where N_{OPC} is the number of OPCs. This enables us to write the parametrically amplified noise (P_{PAN}) and the residual inter channel nonlinearity after compensation with a bandwidth B_{WDM} (P_{NLS}) as;

$$P_{PAN} = \eta P_S^2 P_N \underline{S} \underline{D} \underline{E}$$

$$P_{NLS} = \eta P_S^3 N_T (E_1 - E_2) \quad (6)$$

For the conventional inter channel nonlinear crosstalk, the logarithmic term ($\text{Log}(B^2 / 2f_w^2)$) dominates and $1/\pi$ and $2/\alpha L$ are usually neglected, however when considering digital back propagation the logarithmic and linear terms are equal for back propagation bandwidths of around 15 and 20 GHz (for an 80 km span of standard single mode fibre) respectively and so the linear terms may only be neglected in E_1 for wide WDM bandwidths. Similarly the terms proportional to $\mathbb{H}(\cdot)$ are typically of a similar order of magnitude to N^2 and may only be neglected for the shortest transmission systems.

3. Implications

3.1 Comparison of optical and digital nonlinearity compensation

We consider first three special cases; full bandwidth ($B_{WDM} = B_{DBP}$) transmitter (digital pre-compensation, DPC) and receiver based digital back propagation (DBP) and the use of a single mid-link OPC. In these cases the signal to noise ratio becomes;

$$SNR_{DPC} = \frac{P_S}{NP_N + \eta P_S^2 P_N \left(\left(\text{Log} \left(\frac{B_{WDM}^2}{2f_w^2} \right) + \frac{1}{\pi} - \frac{2}{\alpha L} \right) \frac{N^2 + N}{2} + \frac{2}{\alpha L} (H(N) + N) \right)} \quad (7)$$

$$SNR_{DBP} = \frac{P_s}{NP_N + \eta P_s^2 P_N \left(\left(\text{Log} \left(\frac{B_{WDM}^2}{2f_w^2} \right) + \frac{1}{\pi} - \frac{2}{\alpha L} \right) \frac{N^2 - N}{2} + \frac{2}{\alpha L} (H(N-1) + N) \right)} \quad (8)$$

$$SNR_{OPC-1} = \frac{P_s}{NP_N + \eta P_s^2 P_N \left(\left(\text{Log} \left(\frac{B_{WDM}^2}{2f_w^2} \right) + \frac{1}{\pi} - \frac{2}{\alpha L} \right) \frac{N^2}{4} + \frac{2}{\alpha L} \left(H\left(\frac{N}{2}\right) - \text{Log}\left(\frac{N}{2} - 1\right) + N \right) \right)} \quad (9)$$

where we have emphasized the normally dominant broadband noise term which scales quadratically with length. Noise terms for all three expressions are quadratic in the signal power and so the potential enhancement in signal to noise ratio may be calculated by differentiating Eqs. (7)–(9) with respect to the signal power spectral density. Writing the bracketed terms in the denominator as μ_i , where $i \in \{DPC, DBP, OPC\}$ respectively, the optimum SNR after fully compensating for the inter signal nonlinear effects is given by

$$SNR_i = \left(\frac{3}{2} SNR_0 \right)^{\frac{3}{2}} \left(\frac{\mu_0}{\mu_i} \right)^{\frac{1}{2}} \quad (10)$$

where $\mu_0 = N_T^2 \text{Log} \left(B_{WDM}^2 / 2f_w^2 \right)$. Neglecting the strongly phase matched terms, this implies quite simply that, in the limit of long amplifier chains, digital back propagation may increase the optimum SNR (in dB) by up to 50%, plus an additional 2.64dB. In the case of a mid-point optical phase conjugation, since $\mu_{OPC} \approx \mu_{DBP}/2$ for wide bandwidth signals, the optimum SNR is increased by a further 1.5dB. This is illustrated in Fig. 2, which illustrates the familiar nonlinear threshold curves for an 4,800km system with 5THz continuous signal bandwidth, 80 km spans of standard single mode fibre with coefficients of dispersion, nonlinearity and loss of 17 ps/nm/km, 1.4/W/km, 0.2 dB/km respectively. This figure confirms the potential improvements in signal to noise ratio predicted by Eqs. (6) and (10), arrows represent the simple approximation of a 50% increase in the SNR measured in dB plus the additional 2.64dB, whilst the solid curve represents the full calculation and the dashed curve neglects the strongly phase matched terms. The differences between these three cases are small, but noticeable, as shown by the inset. In the limit of high launch signal power spectral densities, OPC offers a further 3dB improvement in SNR compared to the use of full band DBP, corresponding to a 1.5dB improvement at the optimum launch power.

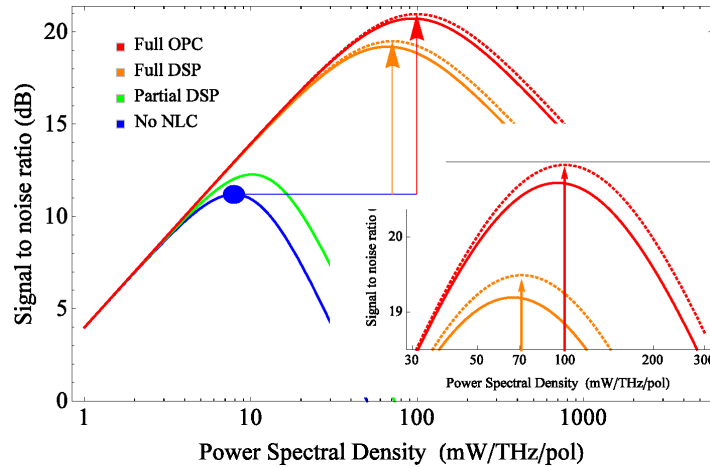


Fig. 2. Nonlinear threshold curves for conventional transmission (blue), ideal digital back propagation (orange) and ideal optical phase conjugation (red) for an 4,800km, 5 THz bandwidth system calculated using Eqs. (5) and (6). Arrows illustrate the approximated signal-to-noise ratio gains predicted by Eq. (10) for large numbers of amplifiers, but neglecting strongly phase matched terms (i.e. $\mu_{\text{DBP}} = \mu_0 = 2, \mu_{\text{OPC}}$). Also shows performance with 300 GHz digital back propagation bandwidth (Green) and the difference between exact (solid) and approximated (dotted) calculations. The inset shows the peaks after compensation on an expanded scale.

Similar results to Fig. 2 are observed for different system lengths, confirming that Eq. (10) predicts the performance improvements with an accuracy of $\pm 1/4$ dB and that OPC should outperform ideal DBP by 1.5dB. For a hybrid system, comprising both DSP and OPC or a system containing multiple OPC devices, we define a normalized signal to noise ratio ΔSNR given by the ratio of the compensated SNR to the SNR with ideal DB. In the case of OPC over an even number of spans with no electronic nonlinearity compensation this value is given by;

$$\Delta\text{SNR} = \frac{\text{SNR}_{\text{OPC}-N_{\text{OPC}}}}{\left(\frac{3}{2}\text{SNR}_0\right)^{\frac{3}{2}}} \approx \sqrt{N_{\text{OPC}} + 1} \quad (11)$$

where $\text{SNR}_{\text{OPC}-N_{\text{OPC}}}$ is the signal to noise ratio after a link comprising N_{OPC} OPC devices. This normalized parameter is largely independent of the system configuration, and may be studied directly to estimate the additional gain over simple digital back propagation ($(\frac{3}{2}\text{SNR}_0)^{3/2}$). Thus, the above equations may be used to optimize the configuration of the nonlinearity compensation.

3.2 Optimization of digital nonlinearity compensation

Figure 3 illustrates the dependence of ΔSNR predicted by Eqs. (5) and (6) for pure DSP based nonlinearity compensation (we assume compensation over the full WDM signal bandwidth and consider the split between transmitter (Eq. (7)) and receiver (Eq. (8))). For all three system lengths considered we firstly observe that the approximate prediction (50% increase in SNR(dB) plus 2.64dB) is reasonably accurate for both full pre compensation and for receiver based digital back propagation. Furthermore, the optimum configuration lies close to an equal split of the processing load between the transmitter and receiver. This optimum is apparent

from the symmetry with respect to the number of DBP stages of the expression in the second and third columns of the matrix \underline{D} . More physically, this optimization corresponds to arranging for undistorted signals to appear at the midpoint of the link and so minimizing the over/under compensation of parametrically amplified noise. We note that similar DSP optimizations towards the center of the link have been observed for alternative nonlinear compensation techniques, such as phase conjugate twin waves [10,28]. The benefit of this split emerges after only two spans (where a midpoint may be correctly defined), and a benefit of approximately 1dB over DBP is rapidly achieved and maintained for a wide range of transmission distances.

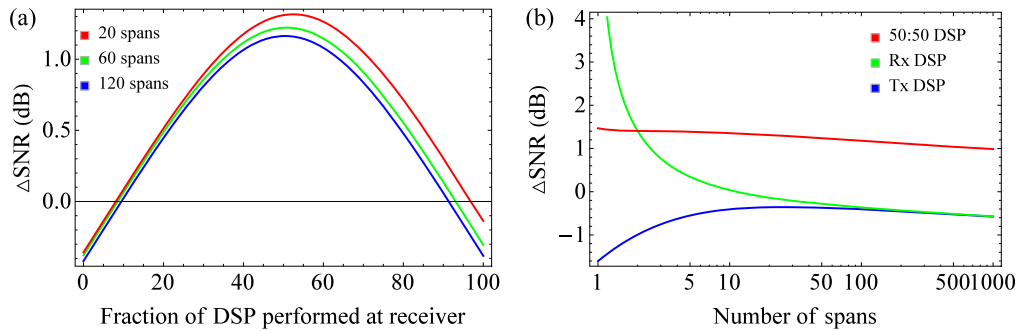


Fig. 3. Optimization of digital signal processing based nonlinear compensation showing (a) the impact of shifting signal processing from the transmitter to the receiver for three different transmission lengths, and (b) the variation in the performance enhancement with system length for three different splits of DSP load. Other system parameters are the same as in Fig. (2). Note

ΔSNR is the change in NLC gain from $\left(\frac{3}{2}\text{SNR}_0\right)^{1/2}$.

The potential impact of implementing nonlinear compensation using optical phase conjugation is illustrated in Fig. 4 for a 120 span system for different numbers of OPC devices. For simplicity we have only plotted results for fully symmetric cases where the lengths of all segments between OPC devices are equal. We have assumed the addition of a variable level of digital back propagation in the receiver, and any transmitter pre-compensation necessary to eliminate inter signal nonlinear penalties, and of course that DSP is performed over the full bandwidth of the WDM signal, and that the nonlinearity compensation from OPC is ideal.

Two key observations are firstly that the inclusion of digital back propagation remains valuable, even when an odd number of OPC devices are used and the intra signal channel interactions are compensated by the OPCs. This is again due to the optimization of the balance between under and over compensating the residual parametric noise amplification. The second observation is that the signal to noise ratio monotonically increases with the number of OPC devices, offering an additional 9dB SNR if ideal OPC devices are placed at each amplifier site. As can be deduced from first two terms of Eq. (6), that is $S_I(D_{11} + D_{12})$ the signal to noise ratio enhancement at the optimum launch power is approximately given by $I + N_{OPC}$. This approximation is plotted as the blue solid line in the inset to Fig. 4. Inclusion of the remaining terms (strong phase matching) gives an excellent agreement (red solid line in inset to Fig. 4). Whilst full summation of Eq. (2) is necessary for accurate results, we would anticipate that the performance of a system with non-uniformly spaced OPC would scale according to the longest segment between two OPCs, which generates the most uncompensated parametrically amplified noise. Non-uniformly spaced OPCs would also have an impact on the function and balance of any DSP implemented in the system. Firstly, the DSP would be required to compensate nonlinearity for any spans without an appropriate conjugate and this could be performed equally well at the transmitter or the receiver.

Secondly, since parametric noise amplification scales approximately quadratically with the number of consecutive spans, we anticipate that the balance between transmitter and receiver DSP should be targeted close to half of the longest run of spans, rather than half of the mean number of spans per segment.

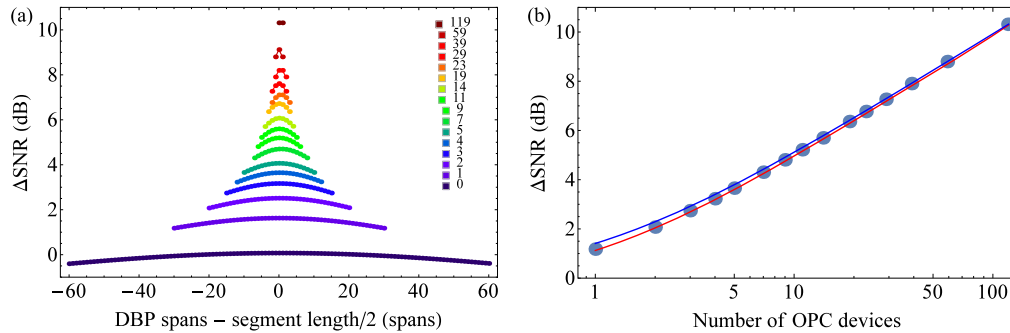


Fig. 4. (a) Increase in signal to noise ratio enhancement for different numbers of OPC devices in a 120 span system, plotted as a function of the number of stages of receiver digital back propagation. Colors represent different numbers of OPC devices as shown in the legend, ranging from no OPC's (bottom curve, corresponding to Fig. 3, left) up to one OPC device per in line amplifier. (b) the SNR improvement as a function of the number of OPC devices, assuming optimized DSP, with approximate (blue) and exact (red) analytical predictions. Note

$$\Delta\text{SNR is the change in NLC gain from } \left(\frac{3}{2} \text{SNR}_0\right)^{3/2}$$

The above discussion suggests that, by segmenting the parametric noise amplification into a number of shorter spans, in line OPC offers an intriguing possibility to significantly enhance the optimum signal to noise ratio of a long haul transmission system, and has a theoretical limit far exceeding that of digital signal processing, where the parametric noise amplification occurs over the whole system length. However, it is well known that there are practical limitations to the implementation of both optical phase conjugation and digital back propagation which would restrict the practically achievable performance. OPC devices themselves are prone to adding additional nonlinear distortions [18], although this penalty scales inversely with pump power [29], especially for highly nonlinear devices, and so we may anticipate resolution of any restrictions within the device itself. The efficiency of the nonlinearity compensation relies on the symmetry of the transmission link. Whilst intensity symmetry may be achieved using either Raman amplification [11] or dispersion pre compensated OPC [30], polarization mode dispersion and third order dispersion may ultimately limit the applicability of this technique over existing fibre links. Resolving these issues will be the subject of a subsequent paper. The main limitation for digital signal processing is the ASIC size and power consumption, which scale super-linearly with the processed bandwidth. For pure DSP based systems this is a severe restriction, and whilst narrow band experiments [31] offer performance enhancement in line with the predictions of Eq. (8), practical implementations offering 1-2 dB enhancement in a fully populated WDM system fall well short of the anticipated 50% increase in signal to noise ratio. Figure 5 shows the impact of DSP bandwidth on a system using OPC. For an even number of OPC devices (including zero) the requirement to compensate for residual inter signal nonlinearity implies that the DSP bandwidth remains a critical parameter, and this is clearly shown by the four curves corresponding to an even number of OPCs (0, 2, 4 and 14) shown. Never-the-less, for even numbers of OPC, the performance improves by up to 4 dB in the case of 14 OPC devices even for a DSP bandwidth of only 50 GHz. For odd numbers of OPC devices, where the inter channel nonlinearity is compensated ideally in the optical domain, and the DSP is only required to compensate for residual parametric noise amplification, the performance improvement becomes significant (as shown in Fig. 4.) and the impact of the DSP bandwidth

is greatly reduced, significant bandwidth increases only resulting in around 1dB performance enhancement. The predicted absolute performance gains are substantial and are reasonably well predicted by Eq. (10) for odd numbers of OPC devices, with the DSP bandwidth dependent offset from this prediction being small (around 1dB) and varying negligibly with the number of OPCs.

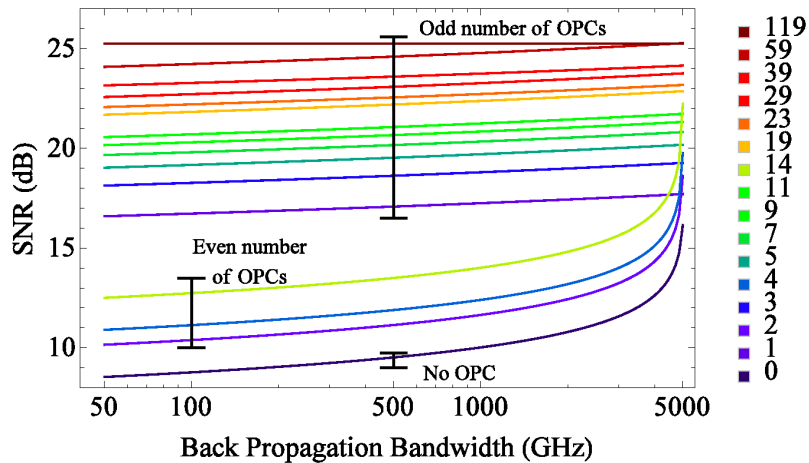


Fig. 5. Impact of DSP bandwidth as a function of the number of OPC devices. System parameters not otherwise specified are as listed in Fig. 2.

4. Numerical verification

In order to verify the predictions of Eq. (9), we carried out numerical simulations of a polarization multiplexed 16QAM Nyquist WDM signal over a transmission span of 2,560km using various number of ideal optical phase conjugation devices, distributed uniformly along the link. The transmitter and transmission link we implemented in Matlab and VPI TransmissionMaker, version 9.3 using with 2^4 samples per symbol per polarisation. In the transmitter 28 Gbaud Nyquist signals with a roll off factor of 0.01 were simulated, with 2^{10} bits per polarization and per wavelength (channel spacing 1.1 times the symbol rate). In order to focus on the effects of parametrically amplified noise, we assumed ideal Raman amplification with zero PMD and dispersion slope. To increase accuracy, Raman noise was added every 2.5km assuming a noise coefficient of 1.13 and a background loss of 0.046 km^{-1} . Ideal OPCs, uniformly distributed along the link, were implemented by reversing the sign of the imaginary field components using a Matlab sub-module. OPC device losses and crosstalk were neglected.

After coherent detection, the receiver DSP was implemented in Matlab. The received signal was down-sampled to 2 samples per bit and the channel of interest extracted using a matched filter. In the absence of OPC, chromatic dispersion was first compensated using a fixed frequency domain equalizer. The signal was the polarization demultiplexed using a 5 tap butterfly filter, optimized using a constant modulus algorithm. Phase recovery was performed using a Viterbi-Viterbi algorithm with an averaging window of 21. Identical DSP parameters were used for all simulations, regardless of the signal to noise ratio or launch power. Performance was estimated from the error vector magnitude, which correlated closely with BER measurements for all configurations where BER measurements were feasible.

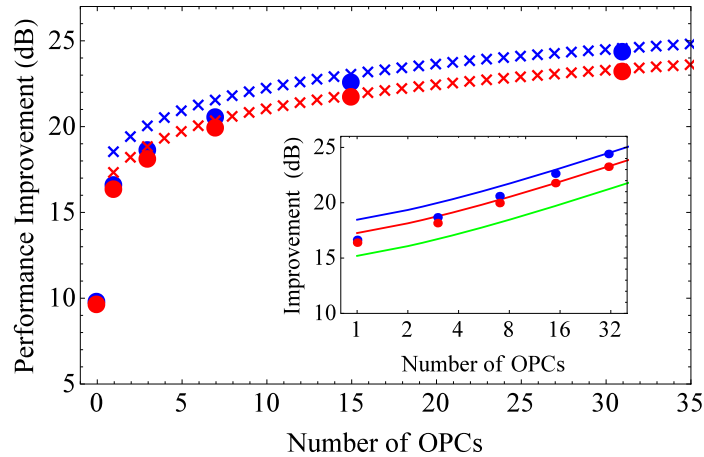


Fig. 6. Performance improvement observed for a variable number of OPC devices considering Eq. (11) (crosses) and a numerically simulated single channel transmission system (filled disks) for single channel (blue), and for 3 channel (red) and full C band (green) WDM systems propagated over a 32x80km of ideal Raman amplified link. Inset shows same data with OPC count shown on a logarithmic scale.

A difference of approximately 2.8 dB between the measured performance/Q-factor and the electrical signal to noise was observed, reflecting the common implementation penalty for 16-QAM Nyquist signals processed at 2 samples per bit. Figure 6 compares the performance of the numerically simulated system with the theoretical prediction of Eq. (11), where a single fitting parameter (SNR_0 for the 3 channel system) was used for all curves. For Raman amplified links, we only consider the bandwidth dependent contributions to the nonlinear noise, since $f_w \rightarrow 0$ as $\alpha \rightarrow 0$ increasing the dominance of this term. Introduction of NLC results in a 7dB performance improvement and the prediction that increasing the number of OPCs enhances the optimum SNR by $\sqrt{2N_{OPC} + 1}$ hold well for 3 channels, and for large numbers of OPCs. This rate of increase is readily observed in the inset to Fig. 6 which plots the data on a log-log scale revealing a straight line whose slope (1/2) may be clearly observed indicating the anticipated power law dependence. Figure 7 shows the power dependent performance of each data point in Fig. 6 along with theoretical fits using Eqs. (8) and (9) where P_N was set to $38\mu\text{W}/\text{THz}$ and η was set to $5.1 \text{ THz}^2/\text{W}^2$. Again, an excellent fit is found between numerical simulations and analytical theory, including in particular an accurate prediction of the nonlinear threshold. As expected from Shannon's theorem, a substantial increase in the optimum launch power is required to realize the benefits of cascaded OPC. We observe that for launch power spectral densities beyond the nonlinear threshold, the rate of decrease in performance is substantially more rapid than would be predicted by Eq. (9). This may be due to uncompensated signal depletion effects [4,32] (neglected in Eq. (1)), higher order nonlinear interactions or sub optimal DSP in this region. The precise cause of this degradation is currently under study, as recent information theory calculations suggest that fiber throughput should increase monotonically with signal power [33].

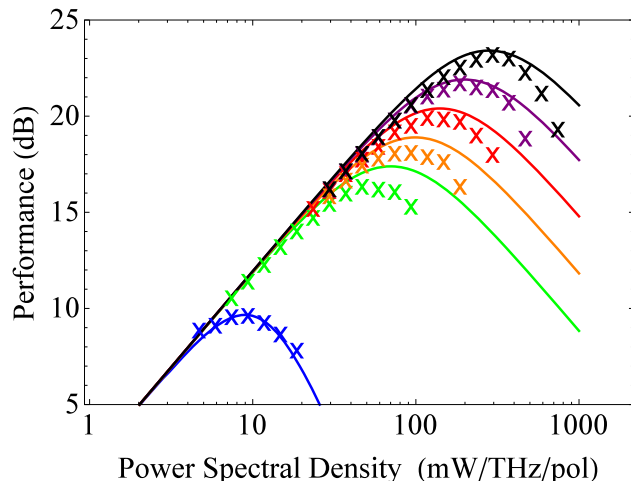


Fig. 7. Comparison of numerically simulated and theoretically predicted performance for a 3 channel WDM transmission comprising ideal Raman amplification and multiple OPCs (number of OPCs: blue-0, green-1, orange-3, red-7, purple-15, black-31).

5. Conclusions

In this paper we have analytically analyzed the impact of multiple optical phase conjugation on an optical transmission system. In addition to the $\sim 50\%$ increase in optimum signal to noise ratio common to all ideal nonlinearity compensation schemes, optical phase conjugation has been shown to interrupt the quadratic growth of parametrically amplified noise. This reduced growth rate enables higher launch powers, and a further increase in optimum signal to noise ratio of $^2\sqrt{N_{OPC} + 1}$, enabling the signal to noise ratio of a long haul system to be more than doubled. We have also shown that the same analytical approach may be used to optimize the distribution of nonlinear compensation between transmitter and receiver DSP and optical phase conjugation, finding that if all inter-channel nonlinearities are compensated optically, the required DSP bandwidth is minimized. For a uniformly spaced OPC system, this optimum performance is obtained when half of a single inter OPC span length is compensated in the transmitter, and half compensated in the receiver (this includes the case of zero OPCs). Assuming such joint nonlinear compensation is applied, we also conclude that an odd number of OPC devices minimizes the required DSP bandwidth.

Acknowledgments

This work was partly funded by The Royal Society (Grant number WM120035) and the Engineering and Physical Sciences Research Council (grant numbers EP/L000091/1 and EP/J017582/1). To access the research data supporting this publication, see <http://www.aston.ac.uk/research/datasets/>.